RSC Polymer Chemistry Series

Edited by Wai-Yeung Wong and Alaa S Abd-El-Aziz

Molecular Design and Applications of Photofunctional Polymers and Materials

RSC Publishing

Molecular Design and Applications of Photofunctional Polymers and Materials

RSC Polymer Chemistry Series

Titles in the Series:
1: Renewable Resources for Functional Polymers and Biomaterials
2: Molecular Design and Applications of Photofunctional Polymers and Materials

How to obtain future titles on publication:
A standing order plan is available for this series. A standing order will bring delivery of each new volume immediately on publication.

For further information please contact:
Book Sales Department, Royal Society of Chemistry, Thomas Graham House, Science Park, Milton Road, Cambridge, CB4 0WF, UK
Telephone: +44 (0)1223 420066, Fax: +44 (0)1223 420247,
Email: booksales@rsc.org
Visit our website at http://www.rsc.org/Shop/Books/

Molecular Design and Applications of Photofunctional Polymers and Materials

Edited by

Wai-Yeung Wong
Department of Chemistry and Centre for Advanced Luminescence Materials, Hong Kong Baptist University, Hong Kong
Email: rwywong@hkbu.edu.hk

Alaa S Abd-El-Aziz
University of Prince Edward Island, Canada

RSC Publishing

RSC Polymer Chemistry Series No. 2

ISBN: 978-1-84973-575-9
ISSN: 2044-0790

A catalogue record for this book is available from the British Library

Published by The Royal Society of Chemistry,
Thomas Graham House, Science Park, Milton Road,
Cambridge CB4 0WF, UK

Registered Charity Number 207890

For further information see our web site at www.rsc.org

Printed in the United Kingdom by Henry Ling Limited, at the Dorset Press, Dorchester, DT1 1HD

Preface

Photofunctional organic and organometallic polymers and materials have become a field of intense activity in optoelectronic/photonic and energy research since they have unique advantages in device fabrication – they are low cost and light weight, offer ease of device fabrication and have potential use in flexible devices. They hold great promise as versatile functional materials for use in energy interconversions. New synthetic methods need to be developed to produce technologically useful materials with specific functional roles. Such research clearly presents a promising way out of the worldwide energy problem. The transformations of light into electricity (*i.e.* electrical energy generation in photovoltaic cells) and electricity into light (*i.e.* light generation in organic light-emitting diodes) are two important interrelated but complementary areas that have attracted considerable research interest in recent years. Work in other optoelectronic, electronic and nanotechnological applications are also emerging rapidly and attract considerable academic and industrial attention. This edited book aims to survey recent research at the frontiers of the topic, with emphasis on fundamental concepts and current applications. Here, a group of experts in the field have made significant contributions to this volume. Other topics such as photochemically degradable polymers, electrochromic and photochromic materials, biosensing and bioimaging materials, and low- and high-refractive index materials are also included. This contribution is very timely and will attract much attention in the scientific community.

Chapter 1, written by Ho and Wong, presents the development of some yellow- and orange-emitting metallophosphors. These phosphorescent dyes find key applications in fabricating monochromatic and white organic light-emitting devices (OLEDs). Chapter 2, by Brady and Tyler, describes some photochemically degradable polymers containing metal-metal bonds and their

RSC Polymer Chemistry Series No. 2
Molecular Design and Applications of Photofunctional Polymers and Materials
Edited by Wai-Yeung Wong and Alaa S Abd-El-Aziz

Published by the Royal Society of Chemistry, www.rsc.org

synthetic and photochemical aspects. The applications of metal acetylide complexes and polymers as photofunctional materials and molecular wires are summarized by Raithby and Long in Chapters 3 and 4, respectively. Chapter 5, by Lo and co-workers, covers the growing field of luminescent transition-metal complexes as biomolecular labels and probes. In Chapters 6 and 7, Nishihara *et al.* first report the exciting area of photoactive metallopolymers whereas Wong and Yam survey the interesting field of photofunctional metal-containing complexes in the latter case. All of these molecules can function effectively as photochromic and optoelectronic materials. In Chapter 8, Mak and co-workers highlight the synthesis and applications of some rhenium(I)-containing polymers. Chapter 9, by Abd-El-Aziz and Strohm, discusses the recent advances in the chemistry of azo-conjugated organometallic and coordination compounds, ranging from small molecules to polymers. Tang *et al.* cover in Chapter 10 the synthesis, characterization and potential photonic applications of some hyperbranched aryleneethynylene polymers. In Chapter 11, Tian and co-workers also nicely present the molecular design of various organic photosensitizing dyes with various donor-π-acceptor-type structures which can be applied in dye-sensitized solar cells, whereas Jin also discusses the related work in Chapter 15 using functional polymers instead of small molecules. A good overview of the recent advances in conjugated polymer nanoparticles is given by Liu *et al.* in Chapter 12, in which they review their different synthetic methods and applications ranging from optoelectronics, cellular imaging to biosensors. In Chapters 13 and 14, Wu and Xie describe some recent studies on polymer-based white light-emitting devices and organic photovoltaic cells, respectively. Within the realm of energy science, both of these topics have important implications towards energy-saving and energy-producing applications.

Clearly, photofunctional materials chemistry represents an intriguing interdisciplinary subject that deserves further research attention in the forthcoming years. Many emerging future challenges as well as opportunities exist for both exploratory and application-oriented research. We are very optimistic to the continuing developments of these light-driven functional materials in the scientific community.

Wai-Yeung Wong
Alaa S. Abd-El-Aziz

Contents

RSC Polymer Chemistry Series No. 2
Molecular Design and Applications of Photofunctional Polymers and Materials
Edited by Wai-Yeung Wong and Alaa S Abd-El-Aziz

Published by the Royal Society of Chemistry, www.rsc.org

CHAPTER 1

Heavy-Metal Organometallic Complexes as Yellow and Orange Triplet Emitters for Organic Light-Emitting Diodes

CHEUK-LAM HO AND WAI-YEUNG WONG*

Institute of Molecular Functional Materials† and Department of Chemistry, Hong Kong Baptist University, Waterloo Road, Kowloon Tong, Hong Kong, P. R. China
*E-mail: rwywong@hkbu.edu.hk
†Areas of Excellence Scheme, University Grants Committee, Hong Kong

1.1 Introduction

While lighting applications account for about 19% of the electricity consumption of the world,[1] the need to reduce energy consumption associated with the low efficiency of conventional lighting systems (*e.g.* the incandescent bulbs) has prompted researchers to pay considerable research attention to developing new energy-saving technologies such as organic light-emitting devices (OLEDs). Actually, incandescent bulbs that have long been the most common lighting sources are very inefficient (converting only 5–10% of this energy into light) and dissipate the main part of the electrical energy absorbed as heat. Even the energy-saving compact fluorescent lamps are only about 20% energy efficient with typical power efficiency of 40–70 lm W^{-1}. Moreover, fluorescent lamps contain a small but significant amount of toxic mercury in the tube,[2] which

RSC Polymer Chemistry Series No. 2
Molecular Design and Applications of Photofunctional Polymers and Materials
Edited by Wai-Yeung Wong and Alaa S Abd-El-Aziz

Published by the Royal Society of Chemistry, www.rsc.org

complicates their disposal and causes an important environmental impact. Recently, the efficiencies of white organic light-emitting devices (WOLEDs) have been shown to approach or surpass those of the fluorescent lamps due to recent advances in novel material synthesis and optimisation of device structures in the past few years.[3,4] The key advantages of OLEDs for flat-panel display applications are their self-emitting property, high luminous efficiency, full colour capability, wide viewing angle, high contrast, low power consumption, low weight, potentially large-area colour displays and flexibility.[5] In particular, recent developments in using phosphorescent materials have led to significant improvements in OLED performance up to 100 lm W^{-1},[6] thus providing organic semiconducting lighting with a very bright future and allowing WOLEDs to become the next generation of light illumination systems.

White-light emission can be obtained based on the principle of additive colour mixing. In practice, this is mostly done by mixing the three primary colours (red, green and blue, RGB). Besides R-G-B phosphorescent emitters, phosphors showing complementary colours, such as blue (B) and orange or yellow (O or Y), can also be utilised to produce white-light emission in the devices. This approach can eliminate the necessity for excessive emissive dopants in a device, hence reducing structural heterogeneities and the device fabrication process can generally be simplified. Building on these attractive properties, research on two-colour WOLEDs still remains scarce and is driving many researchers to investigate high-efficiency yellow or orange triplet emitters.

Of the various heavy-metal ions that could be envisaged for promoting radiative emission of triplet states in OLEDs, iridum(III), platinum(II) and other transition metals have attracted most attention to date. Flourishing studies over the past decade have revealed how the excited-state energies and hence emission colours in several classes of their complexes can be controlled through rational ligand design.[7] Here, we summarise a number of triplet emitters that show yellow or orange electroluminescence (EL) that may serve as good candidates for WOLED applications.

1.2 Iridium(III) Complexes

Iridium(III) complexes are considered to be the seminal generation of phosphorescent emitters. As a general approach, the emission peak wavelength was found to be greatly dependent on the molecular design of the cyclometallating ligand chelates.

1.2.1 Homoleptic and Heteroleptic Iridium(III) Complexes with Modified 2-Phenylpyridyl Moieties

Recently, for OLEDs based on heavy-metal Ir(III) complexes, the benchmark green emitters *fac*-[$Ir(ppy)_3$] and [$Ir(ppy)_2(acac)$][8] (Hppy = 2-phenylpyridine, Hacac = acetylacetone) have drawn great attention due to their ease of synthesis and high efficiency. To generate yellow or orange colour, a very versatile avenue

can be adopted towards emission colour tuning of Ir(III) complexes *via* the facile derivatisation of the phenyl or pyridyl moiety of ppy with various substituents or functionalities. Attachment of the main-group moieties SO_2 and PO to ppy in **Ir-1** and **Ir-2** was reported by Wong *et al.* in which the approach successfully shifts the charge-transfer character from the pyridyl group in some ppy-type complexes to the electron-withdrawing main-group moieties.[9] This kind of complex improves their electron-injection (EI) and electron-transporting (ET) features. The strongly electron-withdrawing inductive influence of the polar PO group in **Ir-2** was shown to lower significantly the lowest unoccupied molecular orbital (LUMO) energy, thus redshifting the emission peak as compared to $[Ir(ppy)_2(acac)]$. **Ir-2** shows a shorter emission wavelength at 541 nm than **Ir-1** (550 nm). The vacuum-deposited yellow-emitting device based on **Ir-1** turned on at 3.7 V, with a maximum luminance (L_{max}) of 48 567 cd m^{-2} at 19.9 V and maximum external quantum efficiency (η_{ext}) of 10.7%, luminance efficiency (η_L) of 35.1 cd A^{-1}, and power efficiency (η_P) of 23.1 lm W^{-1}, while a higher turn-on voltage (12.1 V) was found in the solution-processed yellow-orange device based on **Ir-2** with L_{max} of 7103 cd m^{-2} at 27.9 V and maximum efficiencies of 3.49%, 11.89 cd A^{-1} and 2.40 lm W^{-1}.

By extending the π-electron delocalisation of the aromatic ligand, the energy gap between the ground and lowest excited states can be effectively reduced to provide a redshifted emission. Complexes **Ir-3** to **Ir-7** consist of additional fused aromatic rings either on the phenyl or pyridyl ring of the ppy ligand. Yellow phosphorescence from **Ir-3** exhibits a very broad and featureless peak at *ca.* 550 nm with a wide full spectral width at half-maximum (FWHM) of 87 nm without the formation of excimer emission.[10] It gives high peak forward-viewing η_L, η_P and η_{ext} of 33.6 cd A^{-1}, 21.8 lm W^{-1} and 10.5% along with Commission international de l'Eclairage (CIE) coordinates of (0.45, 0.54). This broad emission and nonexcimer formation effectively overcome the problem of inevitably low colour rendering indexes (CRI) that are common in many WOLEDs. Highly efficient WOLEDs with maximum efficiencies as high as 46 cd A^{-1} and 41 lm W^{-1} under forward voltage bias can be achieved.

3-Phenylisoquinolinyl (**Ir-4** to **Ir-6**)[11] and phenylbenzoquinoline-based (**Ir-7**)[12] Ir(III) complexes also achieve yellow or orange electrophosphorescence.

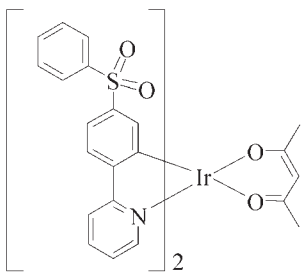

Ir-1

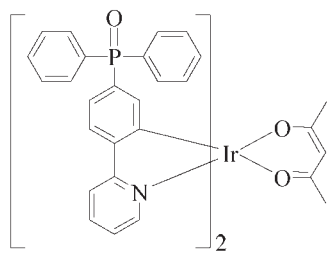

Ir-2

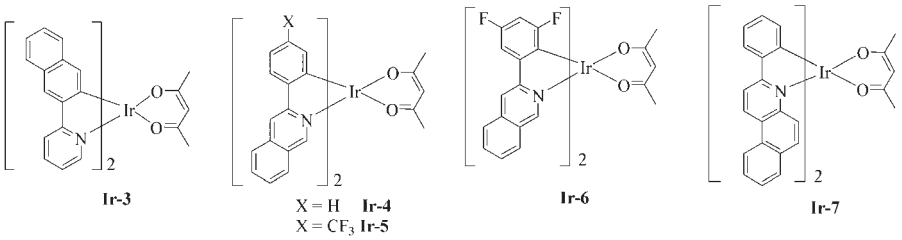

Their corresponding CIE coordinates are (0.49, 0.51), (0.46, 0.53), (0.41, 0.54) and (0.55, 0.44) for **Ir-4** to **Ir-7**, respectively. The better EL performance observed in **Ir-4** can be ascribed to its shorter phosphorescence lifetime. The triplet–triplet (T–T) annihilation becomes more serious for the fluoro derivatives **Ir-5** and **Ir-6**.

Substitution of benzothiazole for pyridine leads to a redshift in the phosphorescence emission. The EL peaks of benzothiazole-based complexes **Ir-8** and **Ir-9** [7e,13,14] appear at around 560 nm in the yellow region and the replacement of S by O in the chromophore causes a blueshift in the emission wavelength to the green region for **Ir-10** due to the lower polarisability and basicity of oxygen relative to sulfur. However, by introducing a CF_3 substituent to **Ir-10**,[15] the phosphor dye emits yellow light at 544 nm with luminance up to 9200 cd m^{-2} at 100 mA cm^{-2}. Orange-emitting OLEDs were also fabricated by using crosslinkable compound **Ir-11**,[16] which can be crosslinked with a hole-conducting matrix *via* cationic ring-opening polymerisation to yield an insoluble emitting layer by using the spin-coating method. The optimal device has a maximum η_L of 18.4 cd A^{-1} at 100 cd m^{-2} and η_P of 11.7 lm W^{-1}. At a luminous density of 1000 cd m^{-2}, the efficiency was still 15 cd A^{-1} and 11.5 lm W^{-1}, respectively. The results gave a performance that compares favourably with other multilayered devices fabricated by thermal evaporation.

Kwon and coworkers designed a Ir(III) complex **Ir-12**[17] with high device efficiency owing to its regulated energy levels and high stability stemming from

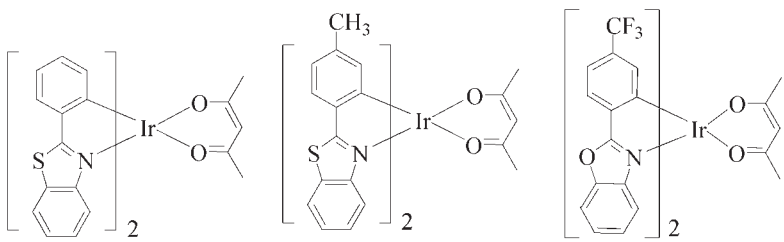

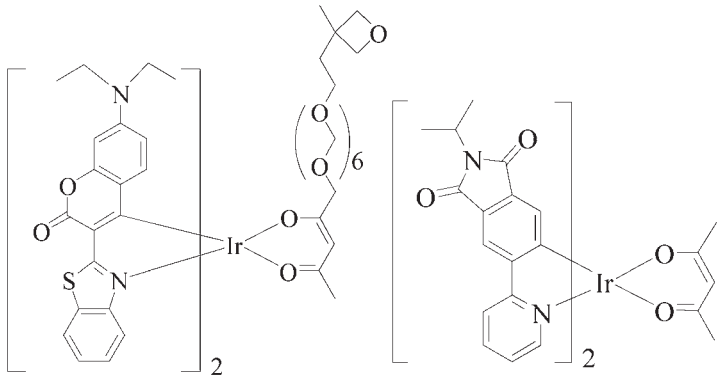

Ir-11 **Ir-12**

the introduction of the imide group as well as the suppressed T–T annihilation in the EL devices in the presence of a bulky isopropyl unit. All the devices with different doping concentrations emit intense orange EL at 566–570 nm with the CIE chromaticity coordinates of (0.51, 0.49) to (0.52, 0.47). The orange-emitting device (λ = 570 nm) with 4 wt.% dopant level exhibited a low operation voltage of 5.3 V at 1000 cd m^{-2}, a maximum η_{ext} of 13.8%, and a maximum η_P of 32.7 lm W^{-1}. Adoption of a double layer-structure enhanced the η_{ext} further to 14.4%.

The use of styrylbenzoimidazole derivatives instead of the traditional pyridine derivatives enhances the ET ability and OLED efficiency at high brightness levels. Devices based on **Ir-13** and **Ir-14** gave yellow EL at 570 and 585 nm, respectively.[18] The performances of the devices based on **Ir-14** are inferior to those of the corresponding devices based on **Ir-13**. The device based on **Ir-13** exhibited a L_{max} of 56 162 cd m^{-2}, accompanied by high η_L of 25.7 cd A^{-1} at high brightness of 1000 cd m^{-2} and 20.7 cd A^{-1} at 10 000 cd m^{-2}.

To investigate the structure–property relationship and develop durable, high-efficiency devices, the groups of Guo and Zou synthesised a series of

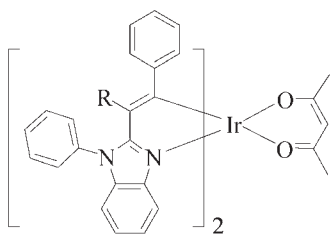

R = H **Ir-13**
CH_3 **Ir-14**

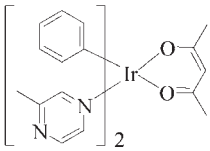

Ir-15

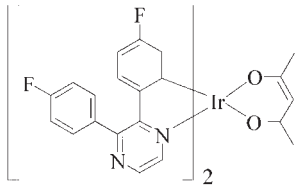

Ir-16

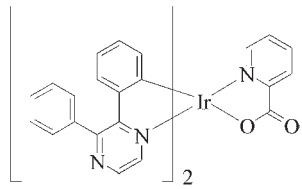

Ir-17

Ir(III) complexes **Ir-15** to **Ir-17** bearing the pyrazine ligands. High yellow colour purity with a featureless emission peak at 580 nm was obtained using **Ir-15**.[19] A systematic study on colour tuning *via* variation of the cyclometallating and ancillary ligands was then carried out. Their phosphorescence peak wavelength can be fine tuned in the yellow range. The emission shifts to the blue in **Ir-16**[20] (λ_{EL} = 561 nm; CIE = (0.45, 0.54)) by adding some fluoro groups to the ligand. The use of picolinic acid instead of acetylacetonate as the ancillary ligand in **Ir-17** also causes a hypsochromic shift in the EL wavelength to 569 nm with CIE of (0.48, 0.50). This result suggests that the strategies for tuning the emission colour and colour purity by changing the ligand substituents can also be applied to the pyrazine system.

The use of a sterically hindered amidinate as the chelating ancillary ligand in **Ir-18** effectively relieves the self-quenching problem in the EL emission and such a group also acts as a good ambipolar charge-transporting material with high hole and electron mobilities.[21] The highest occupied molecular orbital (HOMO) level of this complex is higher than that with acac ligand and therefore the energy gap of **Ir-18** is significantly smaller than that with acac and this can be ascribed in part to the higher π-bonding ability of the amidinate ligand. The better hole-transporting ability of **Ir-18** resulted in excellent EL performance for the orange-emitting device with peak η_{ext} of 18.4%, η_L of 21.4 cd A^{-1} and η_P of 18.7 lm W^{-1}. A WOLED with the structure of ITO/NPB/**Ir-18**:$Bepp_2$/$Bepp_2$/LiF/Al was fabricated ($Bepp_2$ = bis(2-(2-hydroxyphenyl)-pyridine)beryllium, a deep blue-emitting fluorescent complex). The CIE coordinates remain almost unchanged (0.35 $\pm$0.02, 0.33 $\pm$0.02) upon varying the luminance and so the device possesses a high colour reproduci-

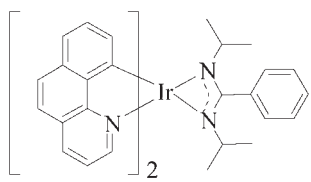

Ir-18

bility. A reasonably low turn-on voltage (2.7 V) was recorded with remarkable EL efficiency at a peak η_{ext} of 27.8% (η_L of 60.8 cd A^{-1}) at a luminance of 300 cd m^{-2} (4.4 V) and the highest η_P of 48.8 lm W^{-1} at 80 cd m^{-2} (3.8 V). Such high performance of the WOLED should be attributed to the carrier direct-injection mechanism as well as efficient energy transfer from $Bepp_2$ to **Ir-18** in the emitting layer.

Devices based on the heteroleptic Ir(III) cyclometallates **Ir-19** and **Ir-20** containing both azolate and diphenylphosphinoaryl chelates displayed bright orange emission.[22] Their photophysical properties are almost identical, regardless of the identity of X and their phosphorescence quantum efficiency can reach near unity for good device performance. The device structure employed was ITO/PEDOT:PSS/NPD/TCTA/host:dopant (10%)/TPBI/LiF/Al (PEDOT:PSS = poly(ethylenedioxythiophene)-poly(styrenesulfonic acid); NPD = *N*,*N*′-di-1-naphthyl-*N*,*N*′-diphenyl-1,1′-biphenyl-4,4′diamine; TCTA = 4,4′,4″-tris(carbazol-9-yl)-triphenylamine; TPBI = 1,3,5-tris[*N*-(phenyl)benzimidazole]benzene). Two different host materials, namely, 4,5-diaza-2′,7′-bis(carbazol-9-yl)-9,9′-spirobifluorene and 4,4′-*N*,*N*′-dicarbazolebiphenyl (CBP), were used for comparison. The results identified that effective energy confinement and appropriate guest–host combinations were observed for the devices using the spirobifluorene-based host that showed higher EL efficiencies with L_{max} of 19 300 cd m^{-2}, η_{ext} = 17.1%, η_P = 49.3 lm W^{-1}, CIE at (0.51, 0.48) for **Ir-19**, and L_{max} of 21 100 cd m^{-2}, η_{ext} = 15%, η_P = 37 lm W^{-1}, CIE at (0.51, 0.49) for **Ir-20**.

Besides modification of the ligand structures, colour tuning was also realised by incorporation of ligands with different electrochemical properties in some heteroleptic coumarin-based structures. Complexes **Ir-21** to **Ir-24** were reported by Ren and coworkers.[23] Due to the fact that coumarin is strongly electron withdrawing and very electron deficient, any replacement of ppy ligands in $Ir(ppy)_3$ with coumarin derivatives can significantly decrease the HOMO energy but it has a less pronounced effect on the LUMO energy, consequently leading to an increased HOMO–LUMO gap and a blueshift in the emission energy. Therefore, the λ_{PL} of **Ir-21** shifts from 550 to 536 nm in **Ir-22**, whereas **Ir-23** shifts from 570 to 544 nm in **Ir-24**. The OLEDs fabricated

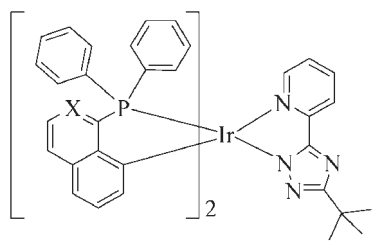

X = CH **Ir-19**
N **Ir-20**

using these coumarin-based Ir(III) complexes as emissive dopants are highly efficient and stable with η_{ext} as high as 20–21% and η_P above 45 lm W^{-1} at 1 mA cm^{-2}. Improved charge balance in the emissive layer was observed in **Ir-21**; thanks to the fact that **Ir-21** is already a good charge-transporting material. Its η_{ext} showed a steady increase as the doping concentration was increased.

Dendrimers are found to be useful in high-performance OLEDs since they can get rid of the lower-purity problem in polymers but can still be processed by solution-based techniques and possess higher thermal properties and glass-transition temperatures than small molecules. To generate yellow EL, Bolink *et al.* synthesised a planar nondelocalised cyclic phosphazene **Ir-25** where the central core is inert, and its optical and electronic properties are dependent on the nature of the dendron, *i.e.* the $Ir(ppy)_3$ fragment in **Ir-25**.[24] This approach is synthetically facile and these rigid spheres can also improve the amorphous properties of the resulting complexes. The EL colour of the device is yellow (CIE coordinates at $x = 0.45$, $y = 0.54$) and becomes redshifted with respect to $[Ir(ppy)_2(acac)]$ (0.31, 0.57), because of elongation of the effective conjugation length *via* the biphenyl unit. The device also provides better results by over 30–35% than that with $[Ir(ppy)_2(acac)]$ fabricated using similar device architectures showing η_L of 24 cd A^{-1} and luminance of 3362 cd m^{-2}.

Single-layer devices were fabricated using charged Ir(III) complex **Ir-26** and it was found to emit yellow light with a brightness that exceeds 300 cd m^{-2} and a luminous power efficiency that exceeds 10 lm W^{-1} at just 3.0 V.[25] Their EL peak maximum varied with the applied bias, and it appeared at 560 nm under forward bias and showed a redshift of 20 nm under reverse bias. The CIE coordinates are $x = 0.425$, $y = 0.549$ for the forward bias and $x = 0.491$, $y = 0.496$ for the reverse one. The PF_6^- space charge was found to dominate the device characteristics.

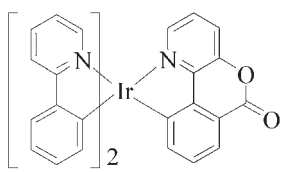

Ir-21

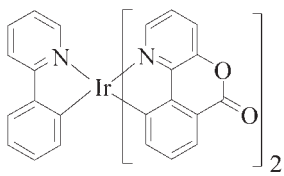

Ir-22

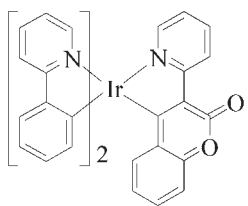

Ir-23

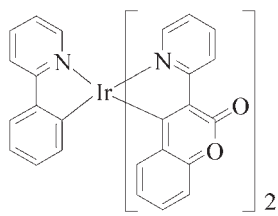

Ir-24

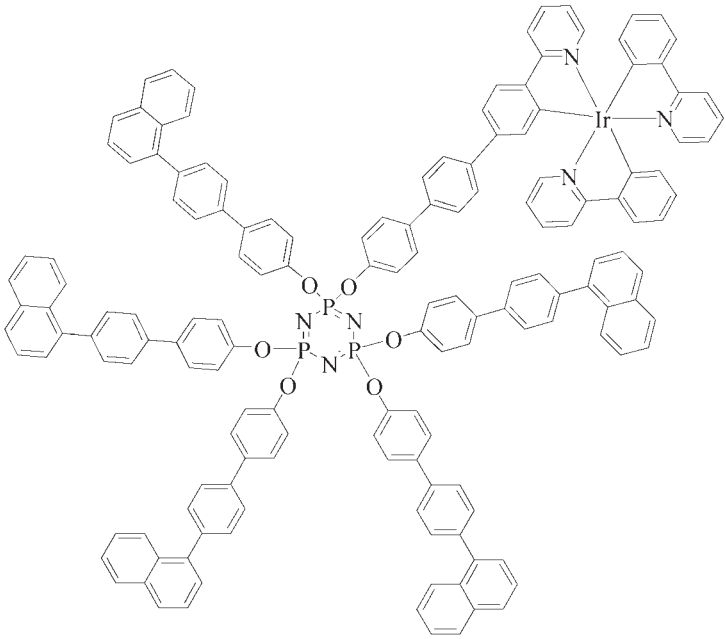

Ir-25

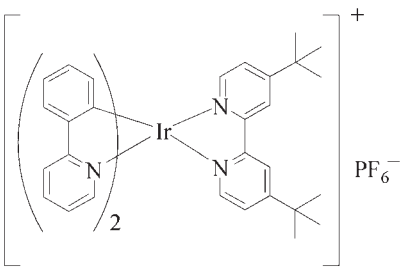

Ir-26

1.2.2 Iridium(III) Complexes Containing Fluorene, Carbazole or Triphenylamine

Recent research endeavours for Ir(III) complexes in OLEDs have involved the use of fluorene-based chromophores, which possess great promise as highly stable and efficient emissive cores in the synthesis of useful Ir(III) complexes. Fluorene-bridged materials possess the advantages of ease of functionalisation at their 9-position of the fluorene ring.[26] By replacing the phenyl ring in $[Ir(ppy)_3]$ with fluorene as for **Ir-27**,[27] the PL peak maximum was largely shifted to 548 nm with a minor shoulder peak at around 588 nm and this

yellow phosphorescence did not show a strong dependence on the dopant level. The apparently yellow emission results from the mixing of green and orange colours in the device. The device at the 2 wt.% doping concentration shows the highest η_{ext} of 10.3%, which corresponds to a peak η_L of 36.7 cd A^{-1} and a η_P of 17.7 lm W^{-1}. The corresponding brightness reached $\sim$ 8190 cd m^{-2} at 12 V and the CIE colour coordinates of 2 wt.% **Ir-27**-doped OLED is (0.44, 0.55), falling into the yellow region of the chromaticity diagram. This promising phosphor was then used to fabricate colour-stable WOLEDs with a four-emission-layer structure. With the optimised device structure and conditions, the highest efficiencies reached 23 cd A^{-1} and 13%, corresponding to a maximum total η_P of $\sim$ 21 lm W^{-1}.

Extension of the π-conjugation through incorporation of electron-rich and hole-transporting carbazole unit in **Ir-28**–**Ir-31**[28] and triphenylamine unit in **Ir-32**–**Ir-33**[29] to the fluorene fragment shows an obvious redshift in their emission profile and destabilises the ground state of the complex by electron donation. This approach increases the HOMO levels and improves the charge balance in the complexes. Better hole injection (HI) and hole transport (HT) were observed in carbazole- or triphenylamine-capped metallophosphors. The HOMO levels are higher for the 3-substituted 9-phenylcarbazole end group than for the *N*-coordinated carbazole unit (*i.e.* **Ir-30** > **Ir-28** and **Ir-31** > **Ir-29**), making the PL peak shift more to the red in the former. They all give intense yellow or orange electrophosphorescene with high EL efficiencies. OLEDs fabricated from multicomponent complexes **Ir-28**–**Ir-31** as the solution-processed emissive layer have been fabricated which showed very high peak efficiencies (9.6%, 29.8 cd A^{-1} and 13.4 lm W^{-1}). Enhanced thermal stability and more morphologically stable amorphous thin-film formation were observed in **Ir-32**–**Ir-33** as compared to **Ir-27**. For optimised orange devices at 5 wt.% of **Ir-33**, the L_{max} reached $\sim$ 45 530 cd m^{-2} at 12 V and the highest η_L is 34.8 cd A^{-1}, corresponding to a peak η_P of 18.2 lm W^{-1} and an η_{ext} of 10.5%.

Work was extended to the ionic metallophosphors as well. **Ir-34** is expected to possess many merits for solid-state lighting and display applications and can show good charge-transfer properties as compared to the neutral species.[30] In spite of the impressive scope that charged complexes can offer in the OLED

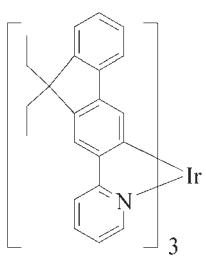

Ir-27

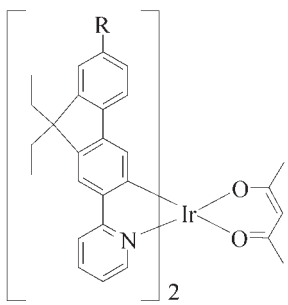

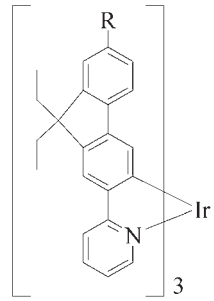

R =

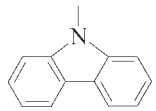

Ir-28

R =

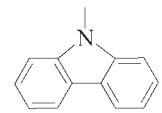

Ir-29

R =

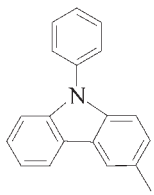

Ir-30

R =

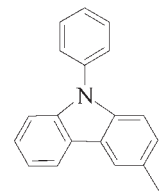

Ir-31

industry, the poor sublimability of charged Ir(III) dopant and its inferior compatibility with common hydrophobic polymer host tends to hinder their widespread practical applications. Interestingly, cationic **Ir-34** coordinated by the HT groups can be vacuum sublimed without significant decomposition to make evaporated orange-emitting OLEDs successfully. Efficient yellow OLEDs doped with 5 wt.% **Ir-34** can be fabricated, showing peak efficiencies of 6.5%, 19.7 cd A^{-1} and 18.4 lm W^{-1} with EL peak maximum at 565 nm. The

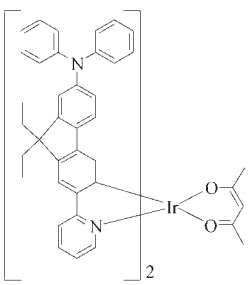

Ir-32

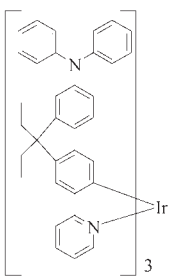

Ir-33

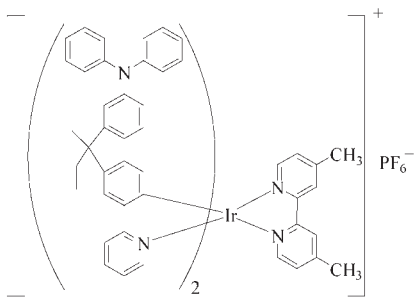

Ir-34

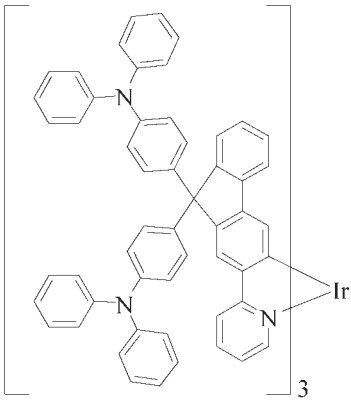

Ir-35

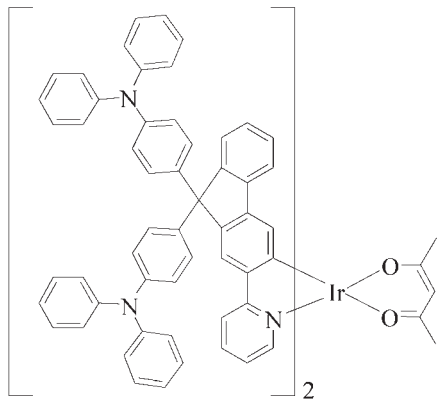

Ir-36

work provides a good platform for developing vacuum-sublimable charged metallophosphors for the design of highly efficient OLEDs and light-emitting electrochemical cells (LECs).

New yellow or yellow-orange Ir(III) triplet emitters with minimised T–T annihilation were reported by Wong and coworkers by functionalisation at the 9-position of fluorene ring. Complexes **Ir-35** and **Ir-36** with two sterically bulky triphenylamine moieties have sufficiently high glass-transition temperature to avoid crystallisation and also prevent close contact between dopant molecules.[31] Both amorphous molecules have the potential of facilitating HI, alleviating the T–T annihilation problem at high current density and hence fabricating simple solution-processible OLEDs even with the use of a small-molecule host only, which makes them good multifunctional phosphorescent materials. Remarkably, efficient and stable OLEDs can be obtained using the configuration of ITO/PEDOT:PSS/x% **Ir-35** or **Ir-36**:CBP/BCP/Alq_3/LiF/Al without the need for a HT layer (BCP: 2,9-dimethyl-4,7-diphenyl-1,10-phenanthroline; Alq_3: tris(8-hydroxyquinolinato)aluminium). The best orange-emitting devices made from **Ir-35** (or **Ir-36**) achieved L_{max} of 25 660 (20 100) cd m^{-2} at 24 (25) V, maximum η_{ext} of 4.63 (6.43)%, η_L of 15.07 (20.42) cd A^{-1} and η_P of 2.36 (3.05) lm W^{-1}. Thanks to the sterically bulky nature of the structure, the roll-off of η_{ext} is only gentle with increasing current density even at the higher doping level. Another way to suppress T–T annihilation and concentration quenching and to improve the film quality is to use a 3-dimensional spirobifluorene core as the cyclometallating ligands, as reported by Chen and his coworkers.[32] Three yellow OLEDs derived from **Ir-37** to **Ir-39** were fabricated by doping the complexes at the concentration of 10 wt.% into the polymeric host material consisting of poly(*N*-vinylcarbazole) (PVK) and 2-(4-biphenylyl)-5(4-*tert*-butyl-phenyl)-1,3,4-oxadiazole (PBD), showing satisfactory device performance. Complex **Ir-37** achieved a peak efficiency of 36.4

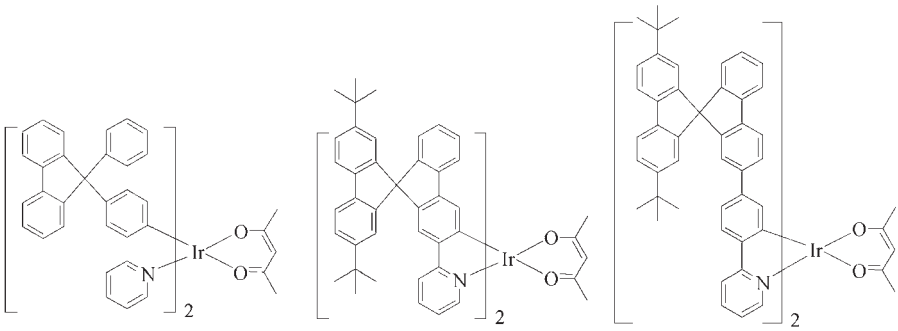

Ir-37 **Ir-38** **Ir-39**

cd A^{-1} (η_{ext} of 10.1%) at 198 cd m^{-2} with λ_{EL} = 555 nm. Extending the electronic conjugation in **Ir-39** shifts the λ_{EL} to 560 nm. The η_{ext} did not decrease obviously with increasing current density, which confirms that the T–T annihilation was largely suppressed by the complexes.

Ir(III) complexes bearing polyphenylene dendritic ligands **Ir-40** to **Ir-42** through simple synthesis and purification procedures are another way to prevent molecular aggregation or $\pi-\pi$ stacking that can show highly efficient EL using solution-processing device fabrication.[33] The emission wavelengths of the materials could be effectively tuned from 549 nm to 582 nm by changing the conjugation of the ligands through incorporating additional aromatic segment (*e.g.* phenyl or fluorenyl group) onto the basic dendritic ligand. The best device performance was achieved by using **Ir-41** as the dopant with the configuration of ITO/PEDOT:PSS (50 nm)/PVK:PBD (40 wt.%):Ir complex (6 wt.%) (70 nm)/ BCP (12 nm)/ Alq_3 (20 nm) / Mg:Ag (150 nm) that gave peak η_L of 34.0 cd A^{-1} and η_{ext} of 10.3%. The efficiencies can be further improved to 46.3 cd A^{-1} and 13.9% if TPBI was used as the charge-blocking layer.

Another approach to achieve yellow EL with functional features such as electron transport (ET) and hole blocking (HB) was achieved using ligand consisting of benzoimidazole unit in the Ir(III) complex (**Ir-43**). The complex emits at λ_{EL} = 568 nm, L_{max} of 21 105 cd m^{-2}, η_{ext} of 7.3%, η_L of 21 cd A^{-1}

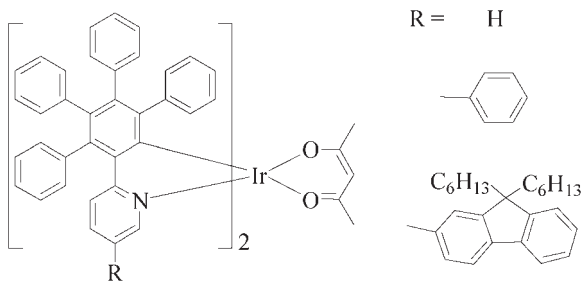

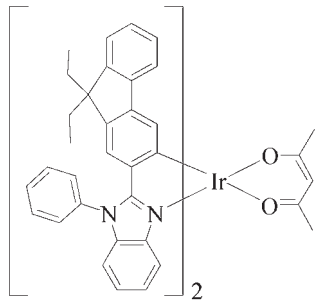

Ir-43

and η_P of 4.7 lm W^{-1} at a current density of 100 mA cm^{-2}, which compare favourably well with those of the green-emitting [$(ppy)_2Ir(acac)$] (λ_{EL} = 525 nm).[7e]

Many research groups have extensively investigated the use of carbazole in the development of new organic electronics materials. Many carbazole-based organic oligomers are high-mobility HT materials that are characterised by tunable and high-energy triplet levels, and they are widely used as the host materials for different metal-organic guests emitting a wide spectrum of visible colours.[34] The robust Ir-carbazolyl complexes have been recognised for their prominent role in ensuring high EL efficiency by elevating the HOMO levels and hence enhancing the HI/HT or hole-trapping features, enhancing the morphological stability as well as EL efficiencies as compared to the ppy and 1-phenylisoquinolinato (piq) congeners.[35] With the bulky, inductively electron-withdrawing CF_3 group on the pyridyl ring in **Ir-44**, an interesting orange electrophosphor (λ_{EL} = 556 nm) was produced that can afford well-performed devices with the highest efficiencies at 40.2 cd A^{-1}, corresponding to η_{ext} of 12.4% and η_P of 24.0 lm W^{-1}. On the other hand, by simply changing the carbazole substitution position from C-3 to C-2 in **Ir-45**,[36] marked changes can be seen in the EL properties, including a redshift of 85 nm in the emission wavelength and a change of the CIE coordinates from green (0.22, 0.60) for C-3 to orange (0.58, 0.39) for C-2. If the carbazole unit is not directly bonded to the metal centre (**Ir-46**), blueshifts of PL and EL spectra were observed that gave rise to yellow emission only.[37]

A multifunctional carbazole-based Ir(III) complex **Ir-47** was reported by Tang *et al.*[38] that contains both a HT carbazole group and an ET oxadiazole group as the main components. This approach was expected to be beneficial to improve the EL performance. Polymer light-emitting diodes (PLEDs) based on a structure of ITO/PEDOT:PSS/PVK:PBD:**Ir-47**/TPBI/CsF/Al were fabricated by solution-processed technology and the resulting EL spectra showed the emission of both monomers and exciplexes. The PLED doped with **Ir-47** at 4 wt.% doping concentration shows the optimal data at L_{max} of 7746 cd cm^{-2},

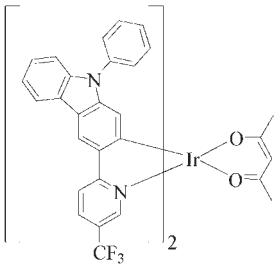

Ir-44

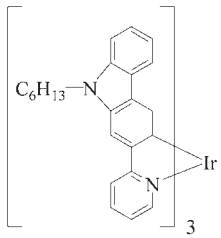

Ir-45

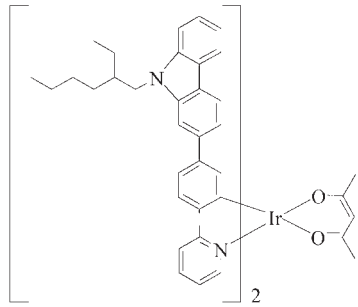

Ir-46

maximum η_L of 14.0 cd A^{-1} and η_{ext} of 5.8% with the CIE coordinates of (0.48, 0.50).

If arylamine groups are linked to 2-phenylpyridine backbone in the Ir complexes (**Ir-48 to Ir-49**),[39] their HOMO levels are shown to be higher compared to [Ir(ppy)$_2$(acac)], therefore an improved HT stability was confirmed. Their EL lies in the orange region of CIE diagram. Due to the increased π-conjugated system of the ligands, the peak emission wavelength of **Ir-49** (λ_{EL} = 589 nm; CIE = (0.58, 0.45)) shows a slight redshift as compared to that of **Ir-48** (λ_{EL} = 581 nm; CIE = (0.54, 0.45)).

The highly amorphous and soluble heteroleptic Ir(III) complex **Ir-50** also experiences a redshift in emission wavelength relative to [Ir(ppy)$_3$] because of the longer conjugation length.[40] The authors believe that there is an efficient interligand energy transfer within the Ir complex. However, a decreased phosphorescence quantum yield (Φ_P) was observed, probably due to the

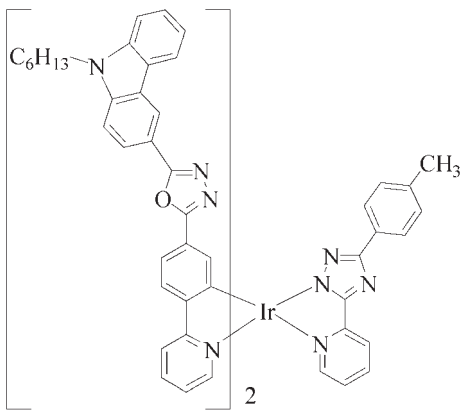

Ir-47

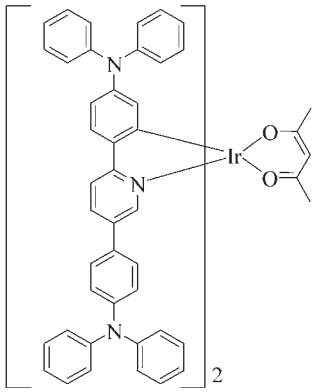

Ir-48

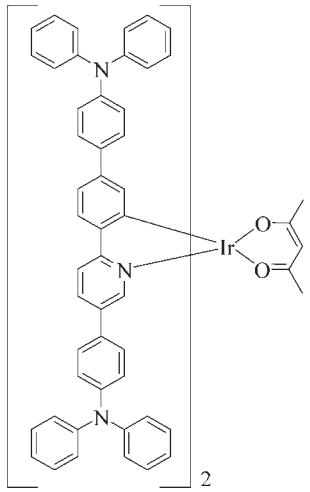

Ir-49

reduced triplet energy of the ligand. The best device performance was obtained with **Ir-50** doped in PVK, which was found to have a L_{max} above 15 000 cd m^{-2} and a peak η_L of 21 cd A^{-1}.

Three phosphorescent dendrimers (**Ir-51** to **Ir-53**) with an Ir(III) complex core and oligocarbazole- or oligofluorene-substituted ligands were reported by Lu and coworkers.[41] Hyperbranched oligocarbazoles or oligofluorenes were attached to the Ir(III) complex core to minimise the interaction between the phosphorescent cores that also functioned as the charge-transporting host for the Ir complex core. The structures of the oligocarbazole were designed to maintain high triplet energy of the ligands so that phosphorescence quenching in the resulting dendrimers can be avoided, while the oligofluorene in **Ir-53**

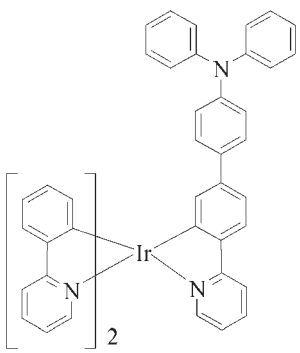

Ir-50

resulted in the unwanted phosphorescence quenching. A strong blue emission from the oligofluorene-substituted ligands besides the emission from the Ir chromophore was observed in **Ir-53** due to the inefficient energy transfer from the oligofluorene-substituted ligands to the Ir(III) complex core. On the contrary, negligible blue emission associated with the oligocarbazole was observed from **Ir-51** and **Ir-52**. Higher PL efficiencies of both of them resulted in better device performance than **Ir-53**. The best performance was obtained from **Ir-52**-based electrophosphorescent OLED with a L_{max} of 13 060 cd m^{-2} and a peak η_L of 4.3 cd A^{-1}, owing to its high PL efficiency and efficient energy transfer between the Ir(III) complex core and the ligands.

1.3 Platinum(II) Complexes

To date, numerous Pt(II) complexes have been used for yellow or orange EL devices. The main striking difference of Pt(II) complexes from the Ir(III) congeners lies in the fact that the emission of the resulting OLEDs may arise from a combination of their own emission as well as the excimeric component in the visible spectrum for the Pt(II) species. Modification of the aryl or pyridyl rings on the Pt(II) ion not only shifts the EL maximum but also makes the white-colour emission possible. This can minimise the complexity of device fabrication in achieving a good white colour balance using multiple emitters instead. Hence, well-balanced EL spectra can easily be obtained in WOLEDs with Pt(II) complexes by employing only one, or at most two dopants showing emission bands of the excimer or exciplex.

There are several types of Pt(II) complexes commonly applied for EL devices. The most common one involves cyclometallated Pt(II) complexes chelated with aromatic pyridyl ligands or similar derivatives and acac as the ancillary ligand. Complexes **Pt-1** and **Pt-2** bearing 2-phenylbenzothiazolate with different substituents were reported by Chen and coworkers[42] For complex **Pt-2** containing the electron-withdrawing fluoro group, it underwent ipsochromic shifts of the PL and EL emissions with respect to the unsubstituted **Pt-1**, inferring that the position occupied by the substituent in the ligand is dominated by the LUMO character. They emit tunable bright yellow-orange light at room temperature (548 and 540 nm for **Pt-1** and **Pt-2**, respectively), and show a bathochromatically shifted emission peak together with the excimer shoulder peak (625–630 nm) with increasing doping concentration. The device with **Pt-2** as the dopant shows relatively better EL performance (L_{max} of 11 320 cd m^{-2} and η_L of 11.3 cd A^{-1}) than that for **Pt-1**.

Efficient fluorescent-based OLEDs were recently reported by using highly fluorescent indolizino[3,4,5-*ab*]isoindoles as the emitting layer.[43] Because of their attractive PL quantum yields that are critical for OLED application, Wudl and coworkers complexed this ligand with Pt(II) ion in **Pt-3**.[44] **Pt-3** with 2-pyridin-2-ylindolizino[3,4,5-*ab*]isoindole (pin) was observed to have high quantum yield of 51% in DMSO at 546 nm, emitting mainly from a ligand-centred triplet π-π* state. Inappreciable degrees of charge-transfer character in

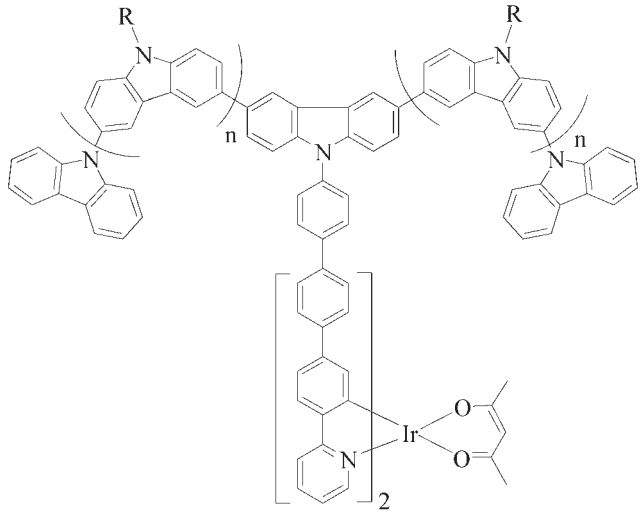

R = n-C_8H_{17}
n = 1 **Ir-51**
n = 3 **Ir-52**

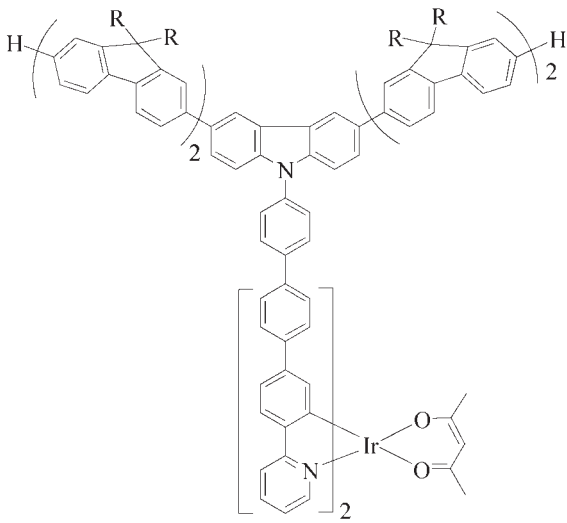

R = n-C_8H_{17} **Ir-53**

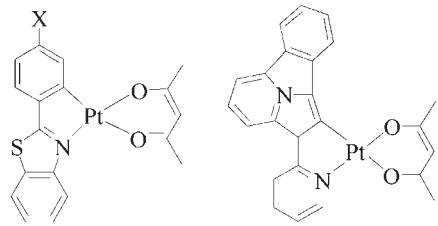

X = H **Pt-1**
X = F **Pt-2**

Pt-3

this complex were confirmed by both the absorption and emission wavelength shifts with the polarity of the solvent used. It is a potential bifunctional emitter because of its relatively low oxidation potential (*ca.* 0.5 V) and this value is among some of the lowest values for other complexes reported.[45] It emits at 553 nm (CIE = 0.46, 0.49) with a FWHM of 63 nm without any aggregation in the EL spectrum.

A novel class of multicomponent neutral complexes **Pt-4** to **Pt-8** was nicely developed recently. **Pt-4**[46] and **Pt-5**[47] bearing carbazole and triphenylamine units exhibit improved thermal or glass-state durability. More importantly, their HI and HT abilities were also improved, catering for more efficient charge transport in their EL process. The introduction of electron-donating carbazole or triphenylamine moiety into the electron-deficient pyridine moiety is expected to increase the electronic conjugation and intramolecular donor–acceptor charge-transfer character of the ligand, causing a redshift in their absorption and emission features as compared to that in [Pt(Fl-py)(acac)] (**Fl-py** = 2-(9,9-diethyl-2-fluorenyl)pyridyl).[47] The greater delocalisation over the aryl ligands also leads to a lesser extent of metal d-orbital mixing and gives a smaller HOMO−LUMO gap, so that both complexes emit in the orange region, while [Pt(Fl-py)acac] emits in the greenish-yellow region. **Pt-4** showed the main emission at 548 nm with a broad shoulder at around 640 nm and revealed a clear aggregation phenomenon as the doping concentration increases. Therefore, the CIE coordinates would vary with a change of concentration and are located at x = 0.49, y = 0.51 at 6 wt.% doping concentration. A maximum η_{ext} of 0.40%, η_P of 0.19 lm W^{-1} and η_L of 1.13 cd A^{-1} were achieved at 3 wt.% doping level. In contrast to many other devices based on similar Pt(II) emitters, however, the problem of aggregation becomes neglectable in **Pt-5**. The devices based on **Pt-5** emit a strong pure orange light with stable CIE colour coordinates of (0.55, 0.45). The use of **Pt-5** suggests a new avenue towards obtaining good colour purity of Pt-based OLEDs by eliminating such drawbacks as strong intramolecular interactions and poor emission colour purity of the cyclometallated Pt(β-diketonato) complexes. The best device performance was achieved with the structure of ITO/NPB/5% Pt:mCP/TPBI/LiF/Al, leading to η_{ext} of 4.65%, η_L of 11.75 cd A^{-1} and η_p of

5.27 lm W^{-1}. Much higher efficiencies were obtained if mCP was replaced by CBP, and a L_{max} of 4195 cd m^{-2}, η_{ext} of 6.64%, η_L of 15.41 cd A^{-1} and η_p of 7.07 lm W^{-1} were achieved. Simple WOLEDs were fabricated by the same research group using **Pt-5** and 9,10-di(2-naphthyl)anthracene (ADN) by replacing 1,3-bis(9*H*-carbazol-9-yl)benzene (mCP) or CBP with ADN. Although the preliminary results are not yet attractive, these single-colour EL devices based on **Pt-5** are good candidate for WOLED applications. A blueshift of the EL peak to 540 nm was observed in the yellow region if two triphenylamine groups are attached at the 9-position of fluorene in **Pt-6**.[31] An encouraging performance with L_{max} of 16 070 cd m^{-2} at 17 V, maximum η_{ext} of 3.36%, η_L of 9.55 cd A^{-1} and η_P of 2.31 lm W^{-1} was detected. T–T annihilation only plays its role at a much higher current density (360 $\pm$85 mA cm^{-2}) at a high doping concentration and it is probably due to its long phosphorescence lifetime (8.2 μs at room temperature).

A novel trifunctional cyclometallated Pt(II) complex **Pt-7** integrating the HT triarylamine, ET oxadiazole and EL metallated group into a single molecule was reported by Wong and coworkers.[48,49] This metal chelate is thermally and morphologically stable with respect to sublimation during the device fabrication. It displays a bipolar character since the LUMO level is lower than the most widely used ET/HB material PBD and comparable to Alq_3, whereas the HOMO is also close to NPD, showing its good HT ability. This molecule was used to fabricate a bilayer vacuum-deposited device of ITO/CuPc/**Pt-7**/Ca/Al in which **Pt-7** acts as the neat emissive film without any ET, HT and EI layers. This device exhibited strong orange-yellow EL at 538 and 578 nm with the CIE coordinates at (0.52, 0.47). The multifunctional nature of **Pt-7** renders it a suitable candidate to act as an efficient dopant-free electrophosphorescent emitter. Further enhancement of the charge transfer within the trifunctional molecule was observed in **Pt-8**, a molecule that incorporates a bulky electron-deficient boron moiety and HT arylamine donor as the cyclometallating chelate.[50] The OLEDs based on this emitter greatly improve the efficiencies by the boron functionality that increases the energy

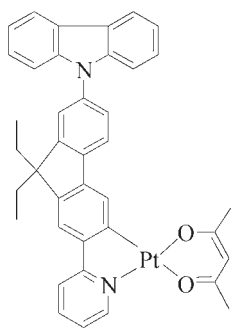

Pt-4

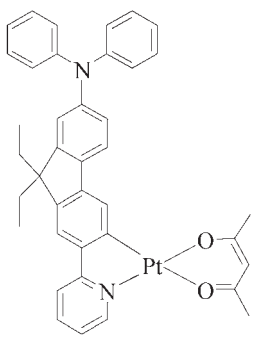

Pt-5

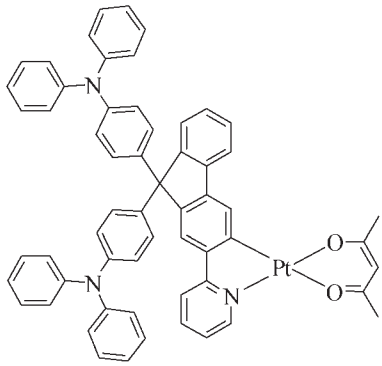

Pt-6

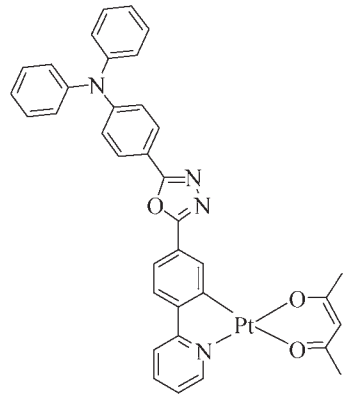

Pt-7

separation between the emissive state and radiatively quenched d-d states, thus providing a large increase in Φ_P and emission brightness despite the large redshift in the emission profile. A remarkably high Φ_P was noted in both the solid ($\Phi_P = 0.46$) and solution ($\Phi_P = 0.91$) states. The highest device efficiency was detected using CBP as the host in the absence of any HB layer. Orange electrophosphorescence peaking at 580 nm (CIE = 0.51, 0.48) was achieved with maximum η_L and η_P of 35.0 cd A^{-1} and 36.6 lm W^{-1} and peak η_{ext} of 10.6%. The result is among the highest reported for a device using a triarylboron-based phosphorescent emitting layer and one of the highest reported using Pt(II) complexes in orange OLEDs.

A good design aimed at colour tuning and suppressing the self-aggregation of Pt(II) complexes is needed to exploit the full potential of Pt(II) emitters. A series of readily sublimable and thermally robust Pt(II) pyridyl azolate complexes (**Pt-9** and **Pt-10**) were prepared by Chang *et al.* that exhibited high structural tuning capability and flexibility at the ligand sites.[51] The steric hindrance from *tert*-butyl and trifluoromethyl functionalities effectively

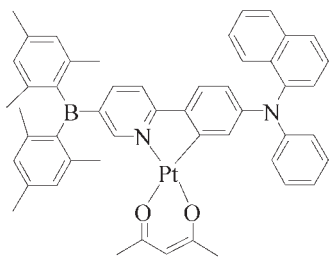

Pt-8

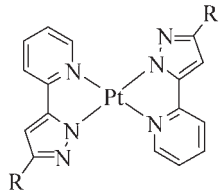

R = t-Bu **Pt-9**
R = CF_3 **Pt-10**

suppresses the self-quenching activities caused by the planar geometry of the Pt(II) complexes and maintains the amorphous property essential for device fabrication. Very bright emissions were observed at all doping concentrations for the multilayer devices with the configuration of ITO/NPB/CBP:**Pt-9**/BCP/Alq_3/LiF/Al. Upon increasing doping concentration, there is an increase in current density and a large redshift in emission maximum. The EL emission shifted from 502 nm (blue-green) to 556 nm (yellow) as the dopant concentration rose from 6% to 100%. A broadening of the emission band was also observed. A similar redshift from 552 nm (yellow) to 616 nm (red) was apparent in the OLEDs fabricated with **Pt-10** with increasing dopant concentration. For emitters such as **Pt-9** that possess ^{3}MLCT/$^3\pi-\pi$ states (MLCT = metal-to-ligand charge transfer), the best device performance was realised using a 6% doping level. The η_{ext} of 2.9%, η_L of 8.6 cd A^{-1} at 20 mA cm^{-2}, and a luminance of 27 114 cd m^{-2} at 15 V were realised. With the emitter **Pt-10** possessing ^{3}MMLCT state (MMLCT = metal-metal-to-ligand charge transfer), the best device performance was achieved at 20% dopant level, along with the η_{ext} of 6.0% and η_L of 19.7 cd A^{-1} both at 20 mA cm^{-2}. These promising results make them remarkable for colour-tuning applications in OLEDs by simply changing the doping concentration of the Pt(II) materials.

Research into the ligand design for EL materials has been dominated by Alq_3 due to its dual function as emissive and ET materials. Attempts to develop alternative quinolinato-substituted Pt(II) complexes **Pt-11** and **Pt-12** for EL applications were made by Che and coworkers.[52] The complexes ligated by tetradentate auxiliaries bis(2′-phenol)-bipyridine and -phenanthroline

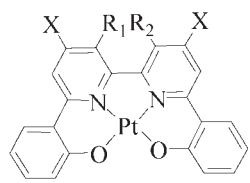

$R_{1,2}$ = HC CH, X = Ph **Pt-11**
$R_1 = R_2$ = H, X = t-Bu **Pt-12**

showed good thermal stability. Both complexes are highly luminescent in solution and display a structureless emission in CH_2Cl_2 at λ_{PL} = 586 and 595 nm, respectively, and the emission properties are influenced by solvent polarity. OLEDs based on 10% of **Pt-11** gave yellow EL and was dominated by its PL at λ_{EL} = 588 nm. Maximum L_{max} and η_P of 850 cd m^{-2} and 0.26 lm W^{-1} were obtained, respectively. Yellow emission (CIE 0.42, 0.56) was also generated for **Pt-12** when its dopant content was increased to 2% with optimal luminance of 4480 cd m^{-2} and η_P of 0.51 lm W^{-1}.

Another family of Pt(II) complexes commonly used for OLED applications are those associated with C^N^N substituted tridentate chelates. They own moderate σ-donating and π-accepting abilities, thus satisfying the demand of the square planar Pt(II) coordination geometry to discourage the D_{2d} distortion that is likely to result in a nonradiative decay and makes them useful in materials design.[53] There are two pathways to fine tune the PL and EL properties of this kind of complexes, namely, modification of the substituent in the C^N^N ligand (**Pt-13**)[54] or attachment of acetylide as the σ-donor ligand with different substituents at the fourth coordination site (**Pt-14**).[55] The donor–acceptor interaction can be strengthened by combining the electron-rich diphenylamine group with the electron-deficient pyridine moiety in **Pt-13**, which shifts the absorption and triplet emission maxima bathochromically to λ_{PL} = 595 nm. The optimal OLED using this complex shows an efficient orange emission with peak maximum at 588 nm and CIE coordinates of (0.570, 0.427) without any voltage-dependence problem. The device turned on at 4.0 V and a luminance of 9000 cd m^{-2} was achieved at 13 V. The peak η_L was shown to be about 11.3 cd A^{-1} and the corresponding η_{ext} is 5.7%. **Pt-14** with the *para*-substituted phenylacetylene shows MLCT PL emission at 582 nm. This is in accordance with the strong σ-donating strength of the alkynyl ligand, which destabilises the dπ(Pt) HOMO to yield relatively low-energy MLCT 5*d*(Pt)→π*(C^N^N) transitions. A L_{max} of 7800 cd m^{-2} at

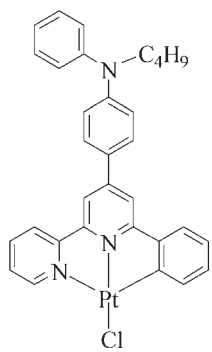

Pt-13

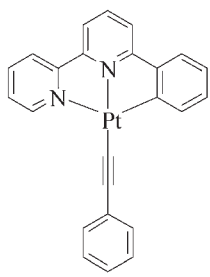

Pt-14

11 V and a maximum efficiency of 2.4 cd A^{-1} at 30 mA cm^{-2} were obtained for an orange-emitting OLED (λ_{EL} = 564 nm) using **Pt-14** at the 4% doping level.

Che also exploited a novel series of naphthyl-substituted cyclometallated C^N^N-type Pt(II) complexes **Pt-15** and **Pt-16** that showed yellow or orange electrophosphorescence.[56] They are strongly emissive, with λ_{PL} depending on the nature of the substituent group R. They possess high thermal stabilities and can be easily sublimed in *vacuo* that render them suitable for application in OLEDs. The devices were fabricated with the architecture of ITO/NPB/Pt dye:CBP/BCP/LiF/Al. For the device containing dopant **Pt-15**, it emitted bright orange light and the EL spectrum showed a peak at 553 nm with a shoulder at 594 nm, and maximum η_{ext} = 12.4%, η_L = 32.3 cd A^{-1} and η_P = 11.2 lm W^{-1} were achieved at a current density of 3.1 mA cm^{-2}, corresponding to a brightness of 1100 cd m^{-2}. The device exhibited a L_{max} of 21 700 cd m^{-2} with excellent colour stability. A better performance was achieved for the device containing dopant **Pt-16**, and it emitted yellow light with a major peak at 540 nm accompanied by a shoulder peak of 580 nm. Maximum η_{ext} = 16.1%, η_L = 51.8 cd A^{-1} and η_P = 23.2 lm W^{-1} were achieved at a current density of 0.44 mA cm^{-2}, corresponding to a brightness of 230 cd m^{-2}. The device exhibited a maximum brightness of 23 500 cd m^{-2} at 16 V and nearly constant CIE coordinates of x = 0.44, y = 0.54.

Another similar class of Pt(II) complexes with O^N^N chelates **Pt-17**–**Pt-21** were reported by the same group.[57] They are robust yellow emitters with good thermal stabilities. Excitation of **Pt-17** to **Pt-21** in DMF solutions resulted in a broad orange-red emission (593–618 nm) at room temperature but blueshifted EL emission bands were observed because of solvent relaxation and doping effects. Their EL maximum is independent of their doping concentration and the device performance follows a trend similar to those for the emission quantum yield and thermal stability (**Pt-21** > **Pt-19** > **Pt-18** > **Pt-20** ~ **Pt-17**). The complex **Pt-21** with bulky *tert*-butyl group and fluoro substituent gave better performance with L_{max} of 37 000 cd m^{-2} and η_L = 7.8 cd A^{-1}.

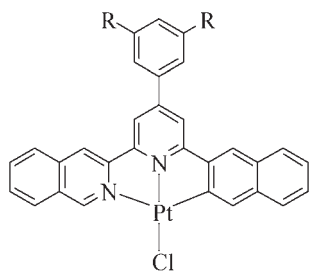

R = CF_3 **Pt-15**
R = t-Bu **Pt-16**

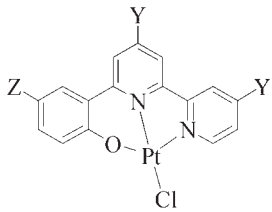

Z = H; Y = Me **Pt-17**

Z = H; Y = H **Pt-18**

Z = H; Y = t-Bu **Pt-19**

Z = F; Y = H **Pt-20**

Z = F; Y = t-Bu **Pt-21**

1.4 Other Metals

Besides Ir(III) and Pt(II) complexes, some other heavy-metal complexes also demonstrate yellow or orange EL bands. The Au(III) alkynyl-based complex **Au-1** with strongly electron-releasing amino substituent was employed as a dopant in multilayer colour-tunable OLEDs.[58] The tunable colour of its EL (from 500 nm to 580 nm upon increasing the dopant concentration) is mainly attributed to the higher order and better packing of the molecules, leading to a stronger π-stacking of the C^N^N ligand and hence resulting in a dimeric or excimeric intraligand EL at the lower energy. Its optimal device gave a L_{max} of 10 000 cd m^{-2}, η_L = 17.6 cd A^{-1}, η_P = 14.5 lm W^{-1} and η_{ext} = 5.5%.

Osmium(II) complexes are also suitable for OLED applications and three orange OLEDs were reported by Shu *et al*. Due to the lower positive charge at the central Os(II) metal cation, the $Os^{2+/3+}$ oxidation is shifted to a lower potential in comparison to the $Ir^{3+/4+}$ couple of its isoelectronic Ir(III) complexes. Likewise, the lowest-energy excited state of Os(II) complexes should contain an increased proportion of the MLCT character. The increase of the MLCT participation may render a significant reduction of its radiative lifetime compared with the respective Ir(III) system and the cathodically shifted oxidation potential pushes up the energy level of HOMO and makes the

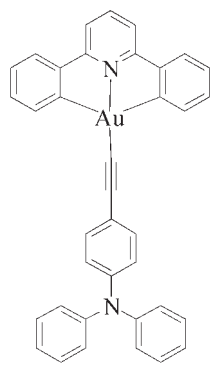

Au-1

neutral Os(II) complexes suitable to serve as the sites for direct charge trapping. In addition, the shortened radiative lifetime reduces the T–T annihilation in the devices, especially at high dopant concentration or higher driving voltage. The solution-processed PLEDs doped with **Os-1** has the EL peak at 602 nm with η_{ext} = 18.7% and η_L = 45 cd A^{-1} and CIE coordinates of (0.58, 0.41).[59] This metallophosphor was also used in combination with a blue fluorescent emitter 4,4′-bis[2-{4-(*N*,*N*-diphenylamino)phenyl}vinyl]biphenyl for the fabrication of WOLEDs. The CIE was recorded at x = 0.33, y = 0.34 at 9.0 V. The short triplet excited state lifetime of **Os-1** (*ca.* 1.0 μs) is beneficial to the remarkable colour stability. This doubly doped device exhibited a pure white-light emission having a high η_{ext} of 6.12% (13.2 cd A^{-1}), and a L_{max} of 11 306 cd m^{-2}. Charge-neutral complexes **Os-2** and **Os-3** can be used to make orange OLEDs using the solution-processing technique.[60] Their emissions appear in the longer-wavelength region and reveal significantly higher quantum yield (**Os-2**: λ_{PL} = 584 nm, Φ_P = 0.80; **Os-3**: λ_{PL} = 572 nm, Φ_P = 0.90). Typical device configurations of ITO/PEDOT/PVK:PBD:Os dye/TPBI/Mg:Ag/Ag were employed. Characteristic emission band at *ca.* 548 nm from **Os-2** and blue emission from PVK/PBD host were totally suppressed, but this is not the case for the **Os-3** based devices, which still presents a substantial amount of the PVK host emission at the 0.4 mol% dopant level. This implies complete Förster energy transfer from the host to the dopant sites in the former case. Increasing the doping concentration of **Os-3** to 1.6 mol% resulted in complete energy transfer and improved the device performance. The maximum η_{ext} of the devices doped with 0.4 mol% of **Os-2** and **Os-3** are 11.7% (40.4 cd A^{-1} at 2.1 mA cm^{-2}) and 11.7% (38.5 cd A^{-1} at 2.2 mA cm^{-2}); whereas the CIE coordinates are located at (0.45, 0.53) and (0.42, 0.52), respectively, and do not show much variation upon changing the applied voltage. By increasing the doping concentration of **Os-3** to 1.6 mol%, the peak η_{ext} reached 13.3% (48.9 cd A^{-1} at 6.3 mA cm^{-2}) with a L_{max} of 28 816 cd m^{-2} at 16 V (96 mA cm^{-2}). The **Os-3**-based device exhibited prominent performance on η_P, which reached as high as 16.8 lm W^{-1} and is 1.7 times higher than that of the **Os-2**-based device due to the significantly lowered driving voltage The use of Os(II) complexes as the active emitting materials in OLEDs should be a

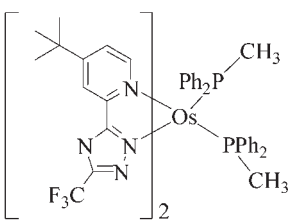

Os-1

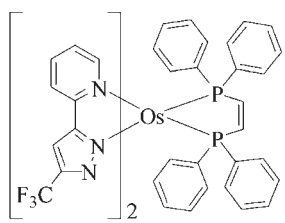

Os-2

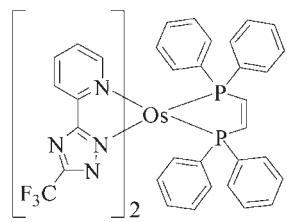

Os-3

valuable option for solid-state lighting applications because of the simple device architecture and the promise of low-cost manufacturability.

1.5 Concluding Remarks

With the aim of optimising the performance of OLEDs, research on the transition-metal complexes evidently still offers great prospects in terms of molecular design and materials properties. In this chapter, we present a library of heavy-metal complexes that can show yellow or orange EL features that are suitable for the development of highly efficient WOLEDs. It is clear that these results should spur new interest to the scientists in the future design and preparation of luminescent materials incorporating heavy transition elements. We are grappling with how to increase the efficiency of these devices (for both monochromatic and white OLEDs) and ensure that they can withstand wear and tear for practical use. We are looking forward these exciting and promising developments with substantial optimism.

Acknowledgements

The authors would like to thank all postgraduate students, postdoctoral associates and collaborators whose names appear in the references. This work was supported by a grant from the University Grants Committee of HKSAR, China (AoE/P-03/08), Hong Kong Research Grants Council (HKBU202709 and HKUST2/CRF/10) and Hong Kong Baptist University (FRG2/10-11/101).

References

1. E. Baranoff, J.-H. Yum, M. Grätzel and M. K. Nazeeruddin, *J. Organomet. Chem.*, 2009, **694**, 2661.
2. C. J. Humphreys, *MRS Bull.*, 2008, **33**, 459.
3. (a) G. Schwartz, M. Pfeiffer, S. Reineke, K. Walzer and K. Leo, *Adv. Mater.*, 2007, **19**, 3672; (b) S.-J. Su, E. Gonmori, H. Sasabe and J. Kido, *Adv. Mater.*, 2008, **20**, 4189.
4. (a) B. W. D′Andrade and S. R. Forrest, *Adv. Mater.*, 2004, **16**, 1585; (b) A. Misra, P. Kumar, M. N. Kamalasanan and S. Chandra, *Semicond. Sci. Technol.*, 2006, **21**, R35; (c) R. F Service, *Science*, 2005, **310**, 1762.
5. (a) S. C. Stinson, *Chem. Eng. News*, 2000, **78**, 22; (b) B. Johnstone, *Technol. Rev.*, 2001, **104**, 80.
6. S. Reineke, F. Lindner, G. Schwartz, N. Seidler, K. Walzer, B. Lussem and K. Leo, *Nature*, 2009, **459**, 234.
7. (a) L. Flamigni, A. Barbieri, C. Sabatini, B. Ventura and F. Barigelletti, *Top. Curr. Chem.*, 2007, **281**, 143; (b) J. A. G. Williams, *Top. Curr. Chem.*, 2007, **281**, 205; (c) Y. Chi and P.-T. Chou, *Chem. Soc. Rev.*, 2010, **39**, 638;

(d) J. A. G. Williams, A. J. Wilkinson and V. L. Whittle, *Dalton Trans.*, 2008, 2081; (e) S. Lamansky, P. Djurovich, D. Murphy, F. Abdel-Razzaq, H. E. Lee, C. Adachi, P. E. Burrows, S. R. Forrest and M. E. Thompson, *J. Am. Chem. Soc.*, 2001, **123**, 4304.

8. M. A. Baldo, M. E. Thompson and S. R. Forrest, *Nature*, 2000, **403**, 750.
9. G. Zhou, C.-L. Ho, W.-Y. Wong, Q. Wang, D. Ma, L. Wang, Z. Lin, T. B. Marder and A. Beeby, *Adv. Funct. Mater.*, 2008, **18**, 499.
10. S.-L. Lai, S.-L. Tao, M.-Y. Chan, M.-F. Lo, T.-W. Ng, S.-T. Lee, W.-M. Zhao and C.-S. Lee, *J. Mater. Chem.*, 2011, **21**, 4983.
11. C.-L. Li, Y.-J. Su, Y.-T. Tao, P.-T. Chou, C.-H. Chien, C.-C. Cheng and R.-S. Liu, *Adv. Funct. Mater.*, 2005, **15**, 387.
12. J. Qiao, L. Duan, L. Tang, L. Wang and Y. Qiu, *J. Mater. Chem.*, 2009, **19**, 6573.
13. W.-C. Chang, A. T. Hu, J.-P. Duan, D. K. Rayabarapu and C.-H. Cheng, *J. Organomet. Chem.*, 2004, **689**, 4882.
14. L. Chen, C. Yang, J. Qin, J. Gao and D. Ma, *Inorg. Chim. Acta*, 2006, **359**, 4207.
15. H.-W. Hong and T.-M. Chen, *Mater. Chem. Phys.*, 2007, **101**, 170.
16. N. Rehmann, C. Ulbricht, A. Köhnen, P. Zacharias, M. C. Gather, D. Hertel, E. Holder, K. Meerholz and U. S. Schubert, *Adv. Mater.*, 2008, **20**, 129.
17. D.-S. Leem, S. O. Jung, S.-O. Kim, J.-W. Park, J. W. Kim, Y.-S. Park, Y.-H. Kim, S.-K. Kwon and J.-J. Kim, *J. Mater. Chem.*, 2009, **19**, 8824.
18. G. Zhang, F. Wu, X. Jiang, P. Sun and C.-H. Cheng, *Synth. Met.*, 2010, **160**, 1906.
19. G. Ge, J. He, H. Guo, F. Wang and D. Zou, *J. Organomet. Chem.*, 2009, **694**, 3050.
20. G. Ge, G. Zhang, H. Guo, Y. Chuai and D. Zou, *Inorg. Chim. Acta*, 2009, **362**, 2231.
21. T. Peng, Y. Yang, H. Bi, Y. Liu, Z. Hou and Y. Wang, *J. Mater. Chem.*, 2011, **21**, 3551.
22. C.-H. Lin, Y. Chi, M.-W. Chung, Y.-J. Chen, K.-W. Wang, G.-H. Lee, P.-T. Chou, W.-Y. Hung and H.-C. Chiu, *Dalton Trans.*, 2011, **40**, 1132.
23. X. Ren, M. E. Kondakova, D. J. Giesen, M. Rajeswaran, M. Madaras and W. C. Lenhart, *Inorg. Chem.*, 2010, **49**, 1301.
24. H. J. Bolink, S. G. Santamaria, S. Sudhakar, C. Zhen and Z. Sellinger, *Chem. Commun.*, 2008, 618.
25. J. D. Slinker, A. A. Gorodetsky, M. S. Lowry, J. Wang, S. Parker, R. Rohl, S. Bernhard and G. G. Malliaras, *J. Am. Chem. Soc.*, 2004, **126**, 2763.
26. (a) D. Neher, *Macromol. Rapid Commun.*, 2001, **22**, 1365; (b) W.-Y. Wong, *Coord. Chem. Rev.*, 2005, **249**, 971.
27. X.-M. Yu, G.-J. Zhou, C.-S. Lam, W.-Y. Wong, X.-L. Zhu, J.-X. Sun, M. Wong and H.-S. Kwok, *J. Organomet. Chem.*, 2008, **693**, 1518.

28. C.-L. Ho, W.-Y. Wong, G.-J. Zhou, B. Yao, Z. Xie and L. Wang, *Adv. Funct. Mater*., 2007, **17**, 2925.
29. (a) W.-Y. Wong, G.-J. Zhou, X.-M. Yu, H.-S. Kwok and B.-Z. Tang, *Adv. Funct. Mater.*, 2006, **16**, 838; (b) X.-M. Yu, H.-S. Kwok, W.-Y. Wong and G.-J. Zhou, *Chem. Mater.*, 2006, **18**, 5097.
30. W.-Y. Wong, G.-J. Zhou, X.-M. Yu, H.-S. Kwok and Z. Lin, *Adv. Funct. Mater.*, 2007, **17**, 315.
31. G.-J. Zhou, W.-Y. Wong, B. Yao, Z. Xie and L. Wang, *J. Mater. Chem.*, 2008, **18**, 1799.
32. J. H. Yao, C. Zhen, K. P. Loh and Z.-K. Chen, *Tetrahedron*, 2008, 10814.
33. C. Huang, C.-G. Zhen, S. P. Su, Z.-K Chen, X. Liu, D.-C. Zou, Y.-R. Shi and K. P. Loh, *J. Organomet. Chem.*, 2009, **694**, 1317.
34. (a) K. Brunner, A. van Dijken, H. Borner, J. J. A. M. Bastiaansen, N. M. M. Kiggen and B. M. W. Langeveld, *J. Am. Chem. Soc.*, 2004, **126**, 6035; (b) S.-J. Yeh, M.-F. Wu, C.-T. Chen, Y.-H. Song, Y. Chi, M.-H. Ho, S.-F. Hsu and C.-H. Chen, *Adv. Mater.*, 2005, **17**, 285; (c) M.-H. Tsai, H.-W. Lin, H.-C. Su, T.-H. Ke, C.-C. Wu, F.-C. Fang, Y.-L. Liao, K.-T. Wong and C.-I. Wu, *Adv. Mater.*, 2006, **18**, 1216; (d) K. R. Justin Thomas, J. T. Lin, Y.-T. Tao and C.-W. Ko, *J. Am. Chem. Soc.*, 2001, **123**, 9404; (e) P. Strohriegl and J. V. Grazulevicius, *Adv. Mater.*, 2003, **13**, 445.
35. (a) W.-Y. Wong, C.-L. Ho, Z.-Q. Gao, B.-X. Mi, C.-H. Chen, K.-W. Cheah and Z. Lin, *Angew. Chem., Int. Ed.*, 2006, **45**, 7800; (b) C.-L. Ho, W.-Y. Wong, Q. Wang, D. Ma, L. Wang and Z. Lin, *Adv. Funct. Mater.*, 2008, **18**, 928; (c) C.-L. Ho, M.-F. Lin, W.-Y. Wong, W.-K. Wong and C.-H. Chen, *Appl. Phys. Lett.*, 2008, **92**, 083301; (d) C.-L. Ho, W.-Y. Wong, Z.-Q. Gao, C.-H. Chen, K.-W. Cheah, B. Yao, Z. Xie, Q. Wang, D. Ma, L. Wang, X.-M. Yu, H.-S. Kwok and Z. Lin, *Adv. Funct. Mater.*, 2008, **18**, 319; (e) C.-L. Ho, Q. Wang, C.-S. Lam, W.-Y. Wong, D. Ma, L. Wang, Z.-Q. Gao, C.-H. Chen, K.-W. Cheah and Z. Lin, *Chem. Asian J.*, 2009, **4**, 89.
36. S. Bettington, M. Tavasli, M. R. Bryce, A. Beeby, H. Al-Attar and A. P. Monkman, *Chem. Eur. J.*, 2007, **13**, 1423.
37. Y. Tao, Q. Wang, C. Yang, K. Zhang, Q. Wang, T. Zou, J. Qin and D. Ma, *J. Mater. Chem.*, 2008, **18**, 4091.
38. H. Tang, Y. Li, B. Chen, H. Wu, W. Yang and Y. Cao, *Opt. Mater.*, 2011, **33**, 1291.
39. D. Wang, J. Wang, H.-L. Fan, H.-F. Huang, Z.-Z. Chu, X.-C. Gao and D.-C. Zou, *Inorg. Chim. Acta*, 2011, **370**, 340.
40. J. Lu, Q. Liu, J. Ding and Y. Tao, *Synth. Met.*, 2008, **158**, 95.
41. Q.-D. Liu, J. Lu, J. Ding and Y. Tao, *Macromol. Chem. Phys.*, 2008, **209**, 1931.
42. I. R. Lasker, S.-F. Hsu and T.-M Chen, *Polyhedron* 2005, **24**, 881.
43. (a) C. J. Tonzola, A. P. Kulkarni, A. P. Gifford, W. Kaminsky and S. A. Jenekhe, *Adv. Funct. Mater.*, 2007, **17**, 863; (b) R. C. Chiechi, R. J. Tseng, F. Marchioni, Y. Yang and F. Wudl, *Adv. Mater.*, 2006, **18**, 325.

44. T. Mitsumori, L. M. Campos, M. A. Garcia-Garibay, F. Wudl, H. Sato and Y. Sato, *J. Mater. Chem.*, 2009, **19**, 5826.
45. W. Lu, C. W. Chan, K. Cheung and C. M. Che, *Organometallics*, 2001, **20**, 2477.
46. C.-L. Ho, W.-Y. Wong, B. Yao, Z. Xie, L. Wang and Z. Lin, *J. Organomet. Chem.*, 2009, **694**, 2735.
47. G.-J. Zhou, X.-Z. Wang, W.-Y. Wong, X.-M. Yu, H.-S. Kwok and Z. Lin, *J. Organomet. Chem.*, 2007, **692**, 3461.
48. W.-Y. Wong, Z. He, S.-K. So, K.-L. Tong and Z. Lin, *Organometallics*, 2005, **24**, 4079.
49. Z. He, W.-Y. Wong, X. Yu, H.-S. Kwok and Z. Lin, *Inorg. Chem.*, 2006, **45**, 10922.
50. Z. M. Hudson, M. G. Helander, Z.-H. Lu and S. Wang, *Chem. Commun.*, 2011, **47**, 755.
51. S.-Y. Chang, J. Kavitha, S.-W. Li, C.-S. Hsu, Y. Chi, Y.-S. Yeh, P.-T. Chou, G.-H. Lee, A. J. Carty, Y.-T. Tao and C.-H. Chien, *Inorg. Chem.*, 2006, **45**, 137.
52. Y.-Y. Lin, S.-C. Chan, M. C. W. Chan, Y.-J. Hou, N. Zhu, C.-M. Che, Y. Liu and Y. Wang, *Chem. Eur. J.*, 2003, **9**, 1264.
53. (a) S.-W. Lai, M. C.-W. Chan, T.-C. Cheung, S.-M. Peng and C.-M. Che, *Inorg. Chem.*, 1999, **38**, 4046; (b) W. Lu, M. C. W. Chan, N. Zhu, C.-M. Che, C. Li and Z. Hui, *J. Am. Chem. Soc.*, 2004, **126**, 7639.
54. D. Qiu, J. Wu, Z. Xie, Y. Cheng and L. Wang, *J. Organomet. Chem.*, 2009, **694**, 737.
55. W. Lu, B.-X. Mi, M. C. W. Chan, Z. Hui, N. Zhu, S.-T. Lee and C.-M. Che, *Chem. Commun.*, 2002, 206.
56. B.-P. Yan, C. C. C. Cheung, S. C. F. Kui, V. A. L. Roy, C.-M. Che and S.-J. Xu, *Appl. Phys. Lett.*, 2007, **91**, 063508.
57. C.-C. Kwok, H. M. Ngai, S.-C. Chan, I. H. T. Sham, C.-M. Che and N. Zhu, *Inorg. Chem.*, 2005, **44**, 4442.
58. K. M.-C. Wong, X. Zhu, L.-L. Hung, N. Zhu, V. W.-W. Yam and H.-S. Kwok, *Chem. Commun.*, 2005, 2906.
59. P.-I. Shih, C.-F. Shu, Y.-L. Tung and Y. Chi, *Appl. Phys. Lett.*, 2006, **88**, 251110.
60. Y.-M. Cheng, G.-H. Lee, P.-T. Chou, L.-S. Chen, Y. Chi, C.-H. Yang, Y.-H. Song, S.-Y. Chang, P.-I. Shih and C.-F. Shu, *Adv. Funct. Mater.*, 2008, **18**, 183.

CHAPTER 2

Photochemically Degradable Polymers; Synthesis of Polymers with Metal–Metal Bonds Along the Backbone Using Click Chemistry

SARAH E. BRADY AND DAVID R. TYLER*

Department of Chemistry, University of Oregon, Eugene, Oregon, USA 97403
*E-mail: dtyler@uoregon.edu

2.1 Introduction

Photochemically degradable polymers[1–6] fall into two general categories: polymers that are intended to degrade and those that are not intended to degrade. Among the former polymers are those used as photodegradable plastics[7] and as photoresists.[8] Virtually every other polymer is in the latter category because every polymer is eventually susceptible to some type of photochemical degradation. Mechanistic knowledge of photochemical degradation processes is helpful in designing new polymers that are intended to degrade and, conversely, in devising strategies to prevent unintended degradation. However, a major problem in designing polymers with specific degradation properties is that the photochemical degradation processes in polymers are mechanistically complicated.[4] This is not to say that the mechanisms are not understood; in fact, many are understood in detail.

RSC Polymer Chemistry Series No. 2
Molecular Design and Applications of Photofunctional Polymers and Materials
Edited by Wai-Yeung Wong and Alaa S Abd-El-Aziz

Published by the Royal Society of Chemistry, www.rsc.org

Rather, the mechanisms are intricate, often involving multiple steps, crosslinking, and side reactions; this makes pinpointing the effects that various environmental and molecular parameters have on the degradation process difficult. For example, one formidable complication is that oxygen diffusion is the rate-limiting step in many photo-oxidative degradations.[9,10] This adds to the intricacy of the analysis because oxygen diffusion rates are frequently time-dependent.[10,11]

To circumvent many of the experimental and mechanistic complexities in the photodegradation process and therefore make it less difficult to interpret data and obtain fundamental insights, we study model polymers with metal–metal bonds along the backbone of the polymer.[12,13] Such polymers are photodegradable because the metal–metal bonds can be cleaved with visible light (eqn (2.1)) and the resulting metal radicals captured with an appropriate radical trap, typically a carbon–halogen bond or O_2 (Scheme 2.1).[12] By studying the photodegradation of these model polymers, we have been able to extract information without the mechanistic complications inherent in the degradation mechanisms of purely organic polymers. For example, metal radicals do not lead to crosslinking, so this complicating feature found in the degradation of other polymers can be avoided.[12] An additional advantage is that the metal–metal bond is a chromophore, and its distinctive absorption bands in the visible region can be used to monitor the photodegradation reactions by electronic absorption spectroscopy. The use of UV-vis methods to quantify and compare the various degradation rates is a time-saving technique because polymer degradation reactions are typically monitored by stress testing, molecular weight measurements, or attenuated total reflection (ATR) spectroscopy, all of which can be laborious and time consuming. The utility of the metal–metal bond-containing polymers in photodegradation studies has been demonstrated in previous investigations into the effects of mechanical stress,[14] polymer morphology,[15] and temperature[16] on polymer photodegradation rates.

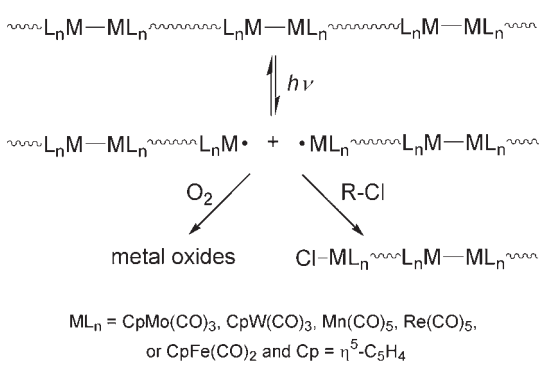

Scheme 2.1 Photochemical reactivity of a polymer with metal–metal bonds along its backbone.

$$L_nM{-}ML_n \xrightarrow{h\nu} L_nM\bullet + \bullet ML_n \tag{2.1}$$

$$\bullet ML_n = CpMo(CO)_3\ (Cp = \eta^5\text{-}C_5H_5),\ CpW(CO)_3,\ Mn(CO)_5,\ Re(CO)_5,\ CpFe(CO)_2$$

In prior papers and reviews, we described metal–metal bond-containing polymers synthesized by step polymerization, chain polymerization, ADMET, and ROMP reactions.[12,13] A recurring problem is that the polymers synthesized by these methods generally have low molecular weights. In order to increase the molecular weight of the polymers and to expand the repertoire of polymer types and morphologies available for study, we have been investigating the use of click chemistry to synthesize polymers. This chapter summarizes some recent work in our laboratory on photochemically degradable polymers synthesized by click reactions. It is important to point out that our research is not necessarily intended to arrive at new commercial photodegradable polymers. Rather, our objectives are to explore the photochemical decomposition mechanisms in various types of polymers (*e.g.*, linear, dendrimers, star, comb, *etc.*) and to explore the effect of environmental and polymer properties on these degradation processes. With this knowledge, we and other workers will be able to design more suitable photodegradable polymers or more suitable light-stable polymers. Before discussing click polymerization reactions, an overview of the methods used to synthesize metal–metal bond-containing polymers is provided. The photochemistry of these polymers is also reviewed.

2.2 Functionalized Metal–Metal Bonded Dimers

Polymers with metal–metal bonds along the backbone have been synthesized using step polymerization, chain polymerization, ROMP, ADMET, and click methods. All of these methods require a functionalized metal–metal bonded dimer as a synthetic starting point, and in our laboratory, we use organometallic dimers with substituted cyclopentadienyl (Cp) rings as the starting materials in these polymerization reactions. A selection of these metal–metal bond-containing synthons is shown in Figure 2.1.[13]

The synthesis of the metal–metal dimers with substituted Cp ligands is challenging due to the weak bond energy of the metal–metal bond ($BDE_{Mo-Mo} \approx 134$ kJ mol^{-1}; $BDE_{W-W} \approx 235$ kJ mol^{-1}).[13] Because the metal–metal bond is relatively weak, the $Cp_2Mo_2(CO)_6$ framework generally cannot withstand the harsh experimental conditions that are necessary to functionalize the Cp ligands. For that reason, it is necessary to synthesize the functionalized Cp ligands first and then coordinate these rings to the metals, followed by formation of the metal–metal bond. Two sample syntheses of metal–metal dimers with substituted Cp ligands are shown in Schemes 2.2 and 2.3.[17] (This synthetic method is emphasized here because it stands in contrast to the methods typically used in the preparation of monomers used to prepare polyferrocenes, perhaps the best-known category of metal-containing poly-

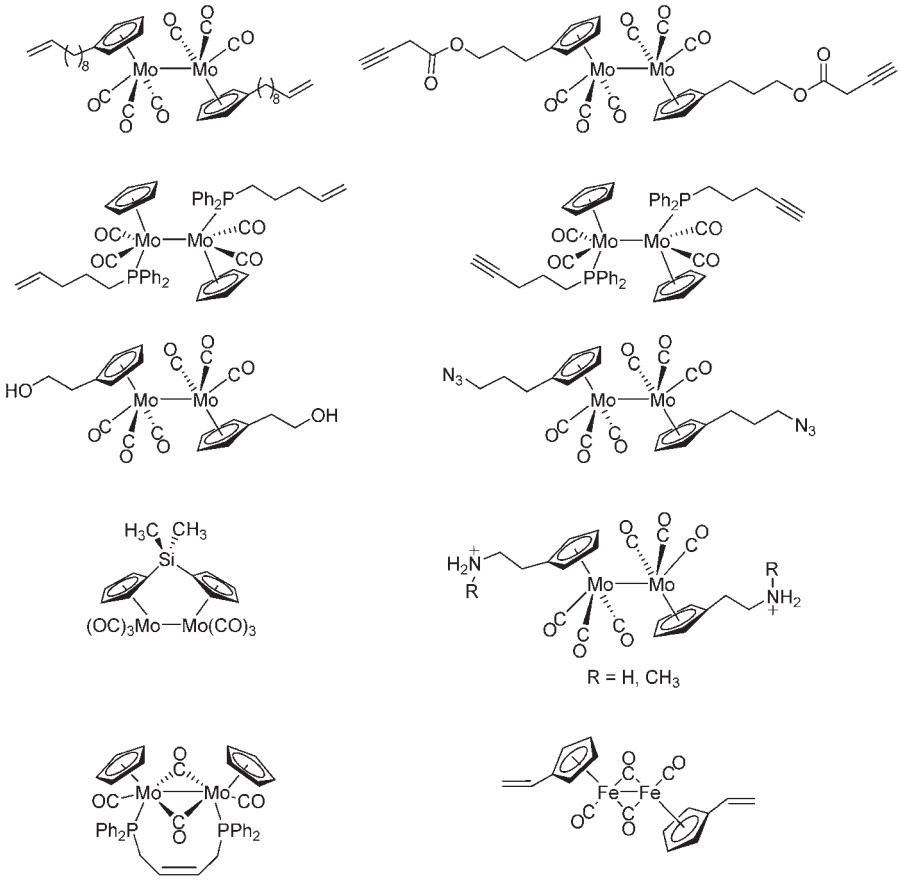

Figure 2.1 Functionalized metal–metal dimers for use in various types of polymerization reactions.

mers. The ferrocene molecule is so robust that the Cp ligands are typically substituted with functional groups after assembly of the Cp_2Fe unit.[18–20]).

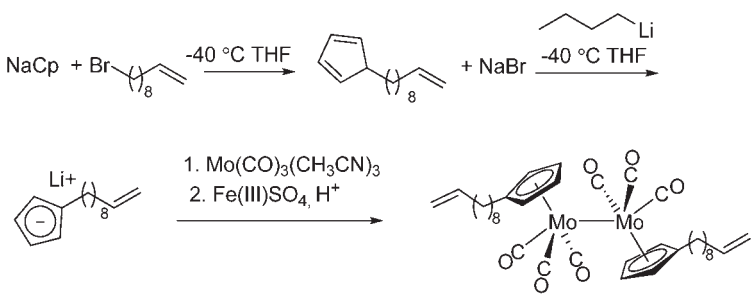

Scheme 2.2 Synthetic route for the preparation of $[(\eta^5\text{-}C_5H_4(CH_2)_8CH{=}CH_2)Mo(CO)_3]_2$.

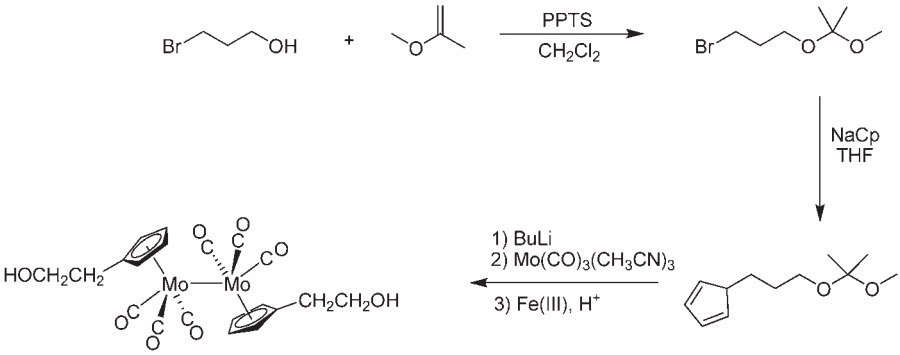

Scheme 2.3 Synthetic route for the preparation of $[(Cp(CH_2)_3OH)Mo(CO)_3]_2$.

2.3 Polymer Syntheses

Just as the comparatively weak metal–metal bonds pose problems for the synthesis of the functionalized-Cp dimers, they cause similar problems in the synthesis of the polymers. The relative weakness of the metal–metal bonds makes them more reactive than the bonds found in standard organic polymers; thus, under many standard polymerization reaction conditions, metal–metal bond cleavage would result. For example, reaction of $(Cp(CH_2)_2OH)_2Mo_2(CO)_6$ with a diacyl halide will typically not yield a high molecular weight polyester because acyl halides can react with metal–metal bonds to form a metal halide complex (eqn (2.2)).[12,21]

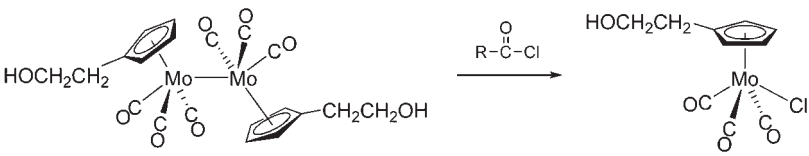

(2.2)

In another example, it is well known that Lewis bases react with metal–metal bonded dimers to form disproportionation products (Mo^{I}-$Mo^{I} \rightarrow Mo^{0} + Mo^{II}$; eq 2.3).[22] Thus, many condensation polymerizations, in which bases are used to neutralize acid condensates, cannot be used in the polymerization reactions involving the metal–metal dimers. To summarize, polymerization reactions that involve metal–metal bonded precursors must generally utilize non-nucleophilic and noncoordinating reagents and solvents, and they must operate under mild reaction conditions. Ideally, they must also be functional group specific. As discussed in the next section, one of the advantages of click chemistry is that these rather stringent reaction conditions are met, and consequently high molecular weight polymers can be obtained.

$$Cp_2Mo_2(CO)_6 + 2\,L \xrightarrow{h\nu} CpMo(CO)_3^- + CpMo(CO)_2L_2^+ + CO \qquad (2.3)$$